The Docking Protein FRS2α Is an Essential Component of Multiple Fibroblast Growth Factor Responses during Early Mouse Development

N. Gotoh,[1,2] K. Manova,[3] S. Tanaka,[4] M. Murohashi,[2] Y. Hadari,[1] A. Lee,[1] Y. Hamada,[5] T. Hiroe,[6] M. Ito,[7] T. Kurihara,[8] H. Nakazato,[8]† M. Shibuya,[2] I. Lax,[1] E. Lacy,[9] and J. Schlessinger[1]*

Department of Pharmacology, Yale University School of Medicine, 333 Cedar Street, New Haven Connecticut 06520[1]; Institute of Medical Science, University of Tokyo, 4-6-1 Shirokane-dai, Minato-ku, Tokyo 108-8639, Japan[2]; Molecular Cytology Core Facility[3] and Developmental Biology Program,[9] Memorial Sloan-Kettering Cancer-Center, 1275 York Avenue, New York, New York 10021; Laboratory of Cellular Biochemistry, Animal Resource Sciences/Veterinary Medical School, University of Tokyo, 1-1-1 Yayoi, Bunkyo-ku, Tokyo 113-8657, Japan[4]; National Institute for Basic Biology[5] and Physiological Science,[6] 38 Myodaizi-machi, Okazaki, Nagoya 444-8585, Japan; Department of Anatomy, National Defense Medical College, 3-2 Namiki, Tokorozawa-shi, Saitama 359-8513, Japan[7]; and Daiichi Suntory Biomedical Research Co., Ltd., 1-1-1 Wakayamadai, Shimamoto-cho, Mishima-gun, Osaka 618-8513, Japan[8]

The docking protein FRS2α is a major mediator of fibroblast growth factor (FGF) signaling. However, the physiological role of FRS2α in vivo remains unknown. In this report, we show that *Frs2α*-null mouse embryos have a defect in anterior-posterior (A-P) axis formation and are developmentally retarded, resulting in embryonic lethality by embryonic day 8. We demonstrate that FRS2α is essential for the maintenance of self-renewing trophoblast stem (TS) cells in response to FGF4 in the extraembryonic ectoderm (ExE) that gives rise to tissues of the placenta. By analyzing chimeric embryos, we found that FRS2α also plays a role in cell movement through the primitive streak during gastrulation. In addition, experiments are presented demonstrating that *Bmp4* expression in TS cells is controlled by mitogen-activated protein kinase-dependent FGF4 stimulation. Moreover, both the expression of *Bmp4* in ExE and activation of Smad1/5 in epiblasts are reduced in *Frs2α*-null embryos. These experiments underscore the critical role of FRS2α in mediating multiple processes during embryonic development and reveal a potential new link between FGF and Bmp4 signaling pathways in early embryogenesis.

A great variety of cellular processes are controlled by the fibroblast growth factor (FGF) family of polypeptide growth factors. FGFs mediate their pleiotropic responses by binding to and activating a family of four receptor tyrosine kinases, designated FGF-receptor 1 to 4 (FGFR1 to -4) (14, 33). Genetic studies have shown that FGFs and FGFRs mediate a variety of cellular responses during embryonic development and in the adult organism (14, 33). In the adult organism, FGF signaling plays a critical role in the control of the nervous system, bone homeostasis, tissue repair, wound healing, and tumor angiogenesis. In addition, FGF signaling plays a critical role in the early stages of embryogenesis (3, 7, 10, 13, 40, 51, 52). While *Fgf4*-null embryos become arrested in their development around the time of implantation, *Fgf8*- and *Fgfr1*-null embryos become arrested later in development due to gastrulation defects caused by impairment in cell movement from the primitive streak (6, 7, 10, 40, 52).

Many of the cellular responses to FGFs are mediated by the membrane-linked docking proteins FRS2α and FRS2β (7, 10, 32, 38, 40, 52). Both proteins contain myristyl anchors and phosphotyrosine binding (PTB) domains in their N termini and multiple tyrosine phosphorylation sites in their C termini that serve as binding sites for the adaptor protein Grb2 and the protein tyrosine phosphatase Shp2 (17, 21). Expression of *Frs2α* begins in the early stages of development, whereas expression of *Frs2β* begins at mid-gestation, predominantly in tissues of neuronal origin (15). The different expression patterns of *Frs2α* and *Frs2β* suggest specific, nonoverlapping roles for each docking protein. Using fibroblasts derived from *Frs2α*-null embryos that do not express FRS2β, we have demonstrated that FRS2α plays an important role in FGF1 stimulation of both the Ras/mitogen-activated protein kinase (MAPK) cascade and the phosphatidylinositol 3-kinase (PI3K)/Akt cell survival pathway (16). However, the physiological role of FRS2α in vivo remains unknown.

After implantation, a mouse embryo develops as a cup-shaped structure, an egg cylinder, with two major layers, the inside ectoderm and the outside visceral endoderm (VE) (4, 46) (see Fig. 7K). The ectoderm is composed of extraembryonic ectoderm (ExE) at the proximal side and epiblast at the distal side. It was proposed that FGF4 secreted from the epiblast mediates the proliferation of multipotent trophoblast stem (TS) cells in the ExE (34, 43).

Emerging evidence indicates that the anterior-posterior (A-P) axis, the first overt manifestation of the body plan, is

* Corresponding author. Mailing address: Department of Pharmacology, Yale University School of Medicine, 333 Cedar Street, New Haven, CT 06520. Phone: (203) 785-7395. Fax: (203) 785-3879. E-mail: joseph.schlessinger@yale.edu.

† Present address: NoviTech Metagenome Research Institute, Ho372-3, Yachimata-shi, 289-1115, Japan.

established when the mouse embryo is at the prestreak stage (4). Several genes, such as *Hex*, are expressed in distal tip VE, and other genes, such as *Brachyury*, are expressed in the proximal epiblast, defining the proximal-distal (P-D) axis. Between embryonic day 5.5 (E5.5) and E6.0, the distal VE tip cells move anteriorward to give rise to the anterior visceral endoderm (AVE), and by E6.5 the proximal epiblast cells move and/or alter gene expression patterns in a posteriorward manner to form the primitive streak. These directional cell movements transform the P-D axis into the A-P axis and can be traced by the shifts in the expression patterns of these genes (41). Signaling pathways stimulated by Nodal, a member of the TGFβ family of cytokines, appear to play a central role in the formation of the P-D axis and the conversion to the A-P axis (30, 48, 54). When the primitive streak appears on the posterior side of the epiblast, gastrulation begins to generate the embryonic and extraembryonic mesoderms.

In this report, we demonstrate that FRS2α deficiency results in impairment in A-P axis and primitive streak formation. Furthermore, FGF4 stimulation of TS cell self-renewal is impaired in *Frs2α*$^{-/-}$ embryos, causing impaired development of the trophobast lineage. Using chimeric embryos, we uncover a role of FRS2α in the control of cell movement through the primitive streak during gastrulation. Finally, we describe a potential new link between FGF and Bmp4 signaling during A-P axis formation in the developing mouse embryo.

MATERIALS AND METHODS

Production of mutant embryos. The *Frs2α*$^{-/-}$ allele has been generated by replacing 22 codons following the ATG codon in the first exon of *Frs2α* gene by a neomycin-resistant gene by homologous recombination (16). Full details about the targeting vector, the strategy for disrupting the *Frs2α* gene, and the characterization of the *Frs2α*$^{-/-}$ allele are described in Hadari et al. (16). The *Frs2α*$^{-/-}$ allele was maintained on a (129sv/EV × Swiss Webster or 129sv/EV) background by intercrossing. Mutants were identified either by their characteristic morphology or by PCR analysis. PCR amplification was carried out using the primer pairs 5′-TCGTGCTTTACGGTATCGCCGC-3′ and 5′-TTAGGTGTTTGCTGCAC TCG-3′ for the mutant allele and 5′-TTTTTGGAGACAGGGTTTCACTG-3′ and 5′-CGCACCTCTGTGCTTTGTAAG-3′ for the wild-type allele. For genotyping of early-stage embryos and TS colonies, the cultured ectoplacental cone, entire embryos or small amount of cells from TS colonies were lysed and genotyped as described previously (20).

Histology and in situ hybridization. Embryos were embedded in plastic resin (JB-4; Polysciences, Inc.) and decidua were embedded in paraffin. Sections 5 to 8 μm thick were used for histological analysis. RNA in situ hybridization was performed as described previously (26), and [^{33}P]UTP was used instead of [^{35}S]UTP to label the probes. Whole-mount RNA in situ hybridization was performed as described previously (15).

Establishment and culture of TS cell lines. TS cell lines were obtained from the blastocysts as described previously (43). TS cell lines were grown in 70% of conditioned medium (EMFI-CM) prepared from the culture of embryonic mouse fibroblasts (EMFI) as described previously (43) and 30% of the TS medium in the presence of FGF4 and heparin.

Immunoprecipitation and immunoblotting. Cells were starved overnight in 1% serum without EMFI-CM and stimulated with FGF1 (100 ng/ml) together with heparin (5 μg/ml) for 10 min at 37°C. Subsequently, the cells were lysed and subjected to immunoprecipitation followed by immunoblotting as described previously (16). Rabbit polyclonal anti-FRS2α antibodies were previously described (20). The other antibodies used in this study are anti-Shp2 antibodies (Santa Cruz; SC-424), anti-phosphotyrosine (phospho) antibodies (PY20; BD Transduction Labs; 610000), anti-Grb2 antibodies (BD Transduction Labs; 610111), anti-phospho-ERK antibodies (Cell Signaling; 9101), and anti-ERK antibodies (Cell Signaling; 9102).

Whole-mount immunohistochemistry. Embryos were fixed in 4% paraformaldehyde at 4°C overnight. The fixed embryos were washed in 0.5% Nonidet P-40 in phosphate-buffered saline (PBS), blocked with PBSST (5% goat serum plus 0.1% Triton X-100 in PBS), and incubated with 1:350 anti-phospho ERK antibodies (Cell Signaling), 1:75 anti-phospho-Smad 1/5/8 antibodies (Cell Signaling), 1:100 anti-ERK antibodies (Cell Signaling), and 1:100 anti-Smad 1 antibodies (UBI) in PBSST. After washing with PBSST, the embryos were incubated with 1:350 biotin-conjugated donkey anti-rabbit antibodies (Jackson) for staining with anti-phospho ERK antibodies, 1:1,000 fluorescein isothiocyanate (FITC)-conjugated goat anti-rabbit antibodies was used (ICN) for staining with anti-phospho-Smad 1/5/8 antibodies or anti-ERK antibodies, and 1:1,000 rhodamine-conjugated goat anti-rabbit antibodies (ICN) was used for staining with anti-Smad 1/5/8 antibodies in PBSST; after incubation, the embryos were washed in PBSST. For staining with anti-phospho ERK antibodies, the embryos were further incubated with 1:1,000 CyX-streptavidin (Jackson) in PBSST and washed with PBSST.

Northern blotting. A group of samples were prepared from the TS cells cultured in TS medium at the indicated time points after removal of FGF4, heparin, and EMFI-CM. The other group of samples were prepared from the TS cells that were cultured in TS medium containing 1% fetal bovine serum (FBS) in place of 20% FBS for 8 h, with or without pretreatment with 50 μM PD98059 for 30 min, and stimulated with FGF4 (100 ng/ml) and heparin (1 μg/ml) for the indicated time. Northern blotting was performed as described previously (43).

Generation of chimeric embryos. In the case of 2N <-> 4N chimeras 4- or 8-cell stage embryos (2N) derived from *Frs2α*$^{-/-}$ intercross matings were aggregated with 4-cell stage tetraploid (4N) ICR embryos. Tetraploid ICR embryos were produced by the electrofusion of embryos at the 2-cell stage as described previously (34). Chimeric embryos which developed into blastocysts within 2 days in culture were transferred to the uterus of pseudopregnant females.

To isolate *Frs2α*$^{-/-}$ ES cell lines marked with a ubiquitous expressed Lac Z marker, *Frs2α*$^{-/+}$ mice (129sv/EV background) were crossed with ROSA26 mice. Two independent *Frs2α*$^{-/-}$ ES cell lines were established as described previously. In the case of *Frs2α*$^{-/-}$ ES <-> 2N chimeras, blastocysts derived from ICR wild-type matings were injected with *Frs2α*$^{-/-}$ ES cells marked with Lac Z.

Bmp4 promoter assay. A genomic fragment containing mouse *Bmp4* gene was as described previously (22). The *Bmp4* 1B promoter and intron 2 promoter used in these studies were as described previously (45). The Bmp4 1A promoter includes nucleotides 34 to 2478 of GenBank accession no. L47480, and the fragment in the 5′-flanking region of the *Bmp4* gene includes nucleotides 53 to 1424 of GenBank accession no. L47480. The sequence of thymidine kinase (TK) minimal promoter was as described previously (25). These fragments were ligated into the firefly luciferase vector (PicaGene Basic vector 2).

TS cells were starved without FGF4, heparin, and EMFI-CM for 12 h and transiently transfected with Lipofectamine 2000 (Invitrogen) in accordance with the manufacturer's instructions. Each well received 0.475 μg of firefly luciferase vector (PicaGene Basic vector 2; TOYO Ink Inc.) carrying fragments of the genome of mouse *Bmp4* gene and 0.1 μg of PicaGene SeaPansy Control vector (pRL-TK) as an internal control. The transfected cells were stimulated with FGF4 (25 ng/ml) and heparin (1 μg/ml) for 24 h and harvested. The transcriptional activity was analyzed with Dual Luciferase Plus Kit (Promega) in accordance with the manufacture's instructions.

RESULTS

To define the phenotype of *Frs2α*-null embryos, we performed a histological examination of embryos from *Frs2α*$^{-/+}$ intercrosses. While embryos were present in most decidua at E5.75, a few decidua had degenerating embryos or empty implantation sites, indicating that a population of mutant embryos likely died immediately after implantation (5/42 decidua, 11.9%) (data not shown). At the onset of gastrulation (E6.5), some empty decidua with implantation sites were detected (4/38 decidua, 10.5%), but the remaining contained embryos with normal morphology. Between E6.75 and E7.5, a mesodermal layer develops between the ectoderm and VE in wild-type embryos, resulting in the formation of three cavities bounded by the amnion and/or chorion (Fig. 1E, G, and I). At E7.0, surviving mutant embryos could be unambiguously identified by their small size (around 30% smaller than wild-type embryos) (Fig. 1A and B). *Frs2α*-null embryos fail to develop a primitive streak but appeared to have mesoderm-like cells
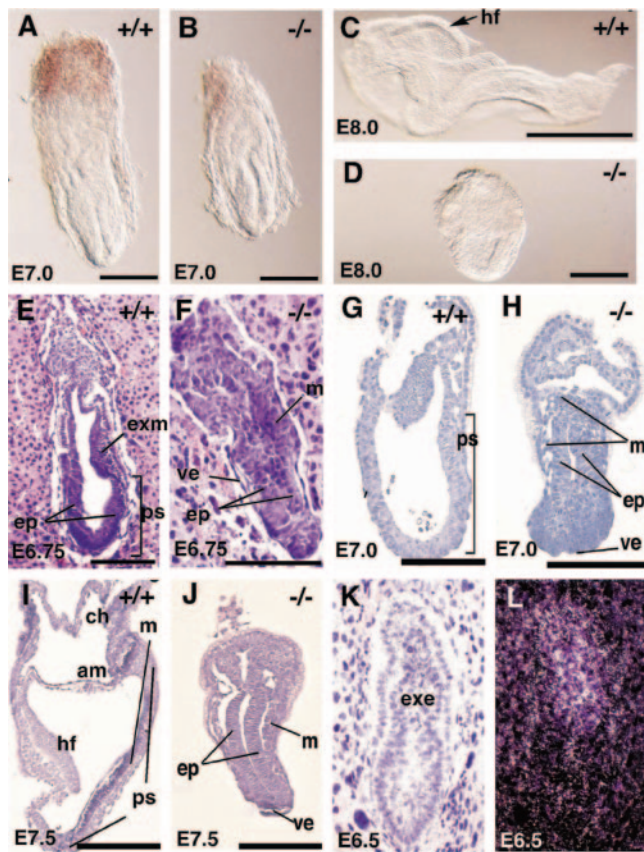
FIG. 1. Morphology and histology of *Frs2α*-null embryos and expression of *Frs2α* at E6.5. Embryonic stage and genotype are indicated for each image. Gross morphology of wild type and mutant embryos (A to D). All embryos are oriented with anterior side to the left. Histological sections of wild-type and mutant embryos (E to J). *Frs2α* mRNA expression in a wild-type embryo at E6.5; bright-field (K) and dark-field (L) images. Hf, head fold; ep, epiblast; exm, extraembryonic mesoderm; ps, primitive streak; ve, visceral endoderm; m, mesodermal cells; ch, chorion; am, amnion; exe, extraembryonic ectoderm. Scale bars, 200 μm.

(Fig. 1F, H, and J). In some mutant embryos, a thickened visceral endoderm was present at the distal region of the egg cylinder (Fig. 1H). By E7.5, *Frs2α*-null embryos are significantly retarded in their development (Fig. 1J). Primitive streak remained deficient, failing to extend (Fig. 1F, H, and J). By E8.0, a few mutant embryos were still present, but they were severely underdeveloped and gradually died (Fig. 1D). Among 79 dissected embryos, 10 mutants (12.7%) were found at E6.75, 24 mutants survived among 154 embryos (15.6%) at E7.5, and only 1 mutant out of 90 examined embryos was found at E8.5 (1.1%). Thus, *Frs2α*-null embryos have a variable phenotype, with approximately half of the mutants dying shortly after implantation, and the remaining half surviving through E7.5 with growth and primitive streak defects.

Since *Frs2α*-null embryos exhibit lethality at early developmental stages, we analyzed the expression of *Frs2α* at E5.5 and E6.5 and found that *Frs2α* is expressed throughout the embryo, with particularly strong expression in the ExE (Fig. 1L and data not shown).

***Frs2α*-null embryos fail to properly establish the A-P axis.** To understand the early mutant phenotype, we examined a panel of molecular markers, using 4 to 5 embryos per probe. First we analyzed the expression of several marker genes diagnostic for proper primitive streak assembly and function between E6.5 and E7.5. While *Brachyury* is expressed in cells ingressing into the primitive streak in wild-type embryos (Fig. 2A and M) (49), the expression of *Brachyury* is confined to a proximal band in the embryonic region of mutant littermates (Fig. 2B and N). Normally, *Lim1* is strongly detected in nascent mesodermal cells moving out of the streak as well as in AVE (Fig. 2C) (39). In contrast, expression of *Lim1*, like that of *Brachyury*, is detected in the proximal region of the mutant embryos (Fig. 2D). *Fgf4* and *Fgf8* also mark the primitive streak in the wild-type embryos (Fig. 2E and G) (9, 29). However, in the mutant littermates at E7.5, *Fgf8* is expressed proximally at a reduced level, while *Fgf4* is expressed throughout the epiblast (Fig. 2F and H). These results indicate that *Frs2α*-null embryos fail to assemble a properly elongating primitive streak in the posterior region; instead, markers of the streak retain a proximal position, one normally found in E5.5 to E6.0 wild-type embryos.

We next examined the expression of anterior-visceral endoderm (AVE) marker genes to assess whether anterior identity is properly specified in the mutant embryos. By E6.0, AVE expression of *Hex*, *Cerberus-related 1* (*Cer-1*), and *Hesx1* is confined to the anterior aspect of wild-type embryos (5, 19, 44), analogous to the pattern shown in Fig. 2I and K. However, even at E6.5, the expression of these genes still has a distal location in *Frs2α*$^{-/-}$ embryos (arrowheads in Fig. 2J and L and data not shown). At the onset of gastrulation, *Otx2* is normally expressed throughout the epiblast and overlying VE; by E7.25 its expression is inhibited posteriorly (Fig. 2O and data not shown) (1). *Otx2* exhibits a similar pattern of expression in wild-type and mutant embryos at the onset of gastrulation. However, by E7.25, as shown in Fig. 2P, *Otx2* is still broadly expressed in the mutants, with transcripts detected in the posterior as well as anterior embryonic regions. Thus, although AVE and posterior marker genes are expressed in *Frs2α*-null embryos, they retain, respectively, their initial distal and proximal positions and fail to acquire the expected anterior and posterior locations found in wild-type embryos.

These experiments show impairment of A-P axis formation in *Frs2α*-null embryos. Since *Frs2α*-null embryos surviving to E6.5 are similar in size to wild-type embryos (Fig. 2I to N and Fig. 3), Frs2α deficiency may first block A-P axis formation in these embryos prior to affecting embryonic growth. Furthermore, since nascent mesodermal cells are produced in mutant embryos (Fig. 1F, H, and J), the block in A-P axis formation does not result from a general developmental arrest at E5.5 to E6.0.

Reduced MAPK activation in the ExE of *Frs2α*-null embryos. To further elucidate the defect in *Frs2α*-null embryos, we analyzed embryos at the pregastrulation stages, before any gross morphological or histological abnormalities are apparent. We analyzed MAPK activation in wild-type and mutant embryos by immunohistochemistry, utilizing antibodies that specifically recognize the activated form of MAPK (anti-phospho Erk). We checked at least 4 litters of embryos including 5 mutants. Consistent with a previous report (8), strong activa-
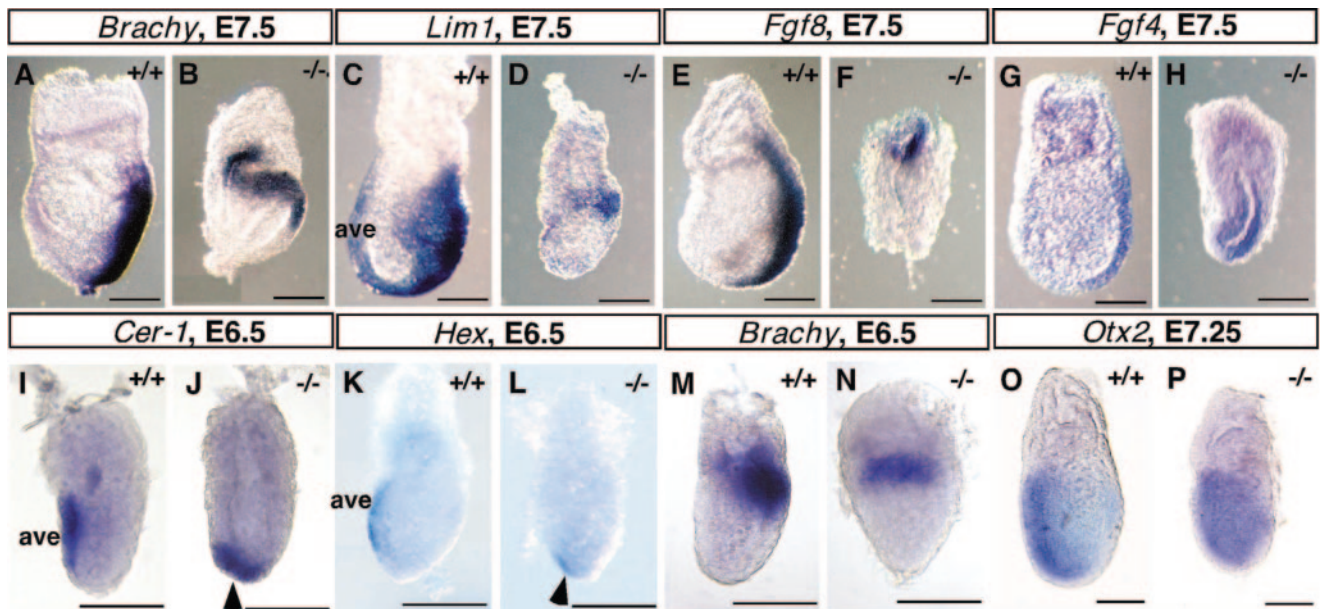
FIG. 2. Expression of marker genes in *Frs2α*-null embryos at gastrulation stages. Embryonic stage, genotype, and marker gene are indicated for each image. All embryos are oriented with anterior side to the left. Scale bars, 100 μm.

tion of MAPK is found in a rim of distal ExE cells adjacent to the epiblast in wild-type and heterozygous embryos (Fig. 3B and D). In contrast, only weak activation of MAPK is observed in mutant embryos (Fig. 3H and J). The reduction in MAPK activation is not caused by impaired development of the ExE and epiblast in egg cylinder stage mutants, as a similar amount and distribution of nonphosphorylated MAPK was found in wild-type and mutant embryos, as revealed by immunostaining with anti-MAPK antibodies (data not shown). These results demonstrate that FRS2α plays a critical role in MAPK activation in the ExE.

TS cell viability requires FRS2α-mediated FGF4 signaling. To further explore the potential impairment of ExE caused by FRS2α deficiency, we tried to establish TS cell lines from the *Frs2α*-null blastocysts. TS cell lines can be isolated from blastocysts by culturing them in the presence of FGF4 (43). Since all presumptive mutants had implantation sites, they should survive beyond the blastocyst stage. We isolated 19 blastocysts from *Frs2α*$^{-/+}$ intercrosses and cultured them individually in the presence of FGF4. All blastocysts became attached to the dish and were cultured for 4 days. After one passage, colonies of TS cells with a tight epithelial morphology appeared (Fig. 4A, upper panel). In 14 of the 19 dishes, TS cells developed well and continued to proliferate after more than 5 passages. However, TS colonies failed to develop in the remaining 5 dishes (Table 1). PCR analysis revealed that these five dishes were seeded with presumptive *Frs2α*$^{-/-}$ blastocysts (Table 1 and Fig. 4A, lower panel). These experiments demonstrate that FRS2α is required for maintenance of TS cells in response to FGF4.

To verify that FRS2α mediates FGF4 signaling in TS cells, we analyzed tyrosine phosphorylation of FRS2α and FRS2α complex formation with Grb2 and Shp2 in response to FGF4 stimulation. Lysates from unstimulated or FGF4-stimulated wild-type TS cells were subjected to immunoprecipitation with

anti-FRS2α or anti-Shp2 antibodies, followed by immunoblotting with anti-phosphotyrosine, anti-Shp2, or anti-Grb2 antibodies (Fig. 4B). The experiment presented in Fig. 4B shows that FGF4 stimulation of TS cells induced tyrosine phosphorylation of FRS2α as well as complex formation between FRS2α and Grb2 and Shp2. Immunoblotting with anti-phospho-Erk antibodies shows that MAPK was activated upon FGF4 stimulation of these cells (Fig. 4B). Taken together, these results argue that a FRS2α deficiency in egg cylinder stage mutant embryos impairs the development and differentiation of the ExE by preventing FGF4 signaling in TS cells.

Analysis of chimeric embryos reveals a primary defect in extraembryonic tissues of *Frs2α*-null embryos and a role for *Frs2α* in cell movement through the primitive streak. If the primary defect in the *Frs2α*-null embryos resides in ExE, then the block in A-P axis formation should be rescued in chimeras constructed by aggregation of *Frs2α*$^{-/-}$ diploid embryos with wild-type tetraploid embryos (*Frs2α*$^{-/-}$ 2N <-> *Frs2α*$^{+/+}$ 4N). The tetraploid cells will exclusively colonize the extraembryonic tissues, namely the ExE and visceral and parietal endoderms, while diploid cells will colonize both the epiblast and extraembryonic tissues (28). Four- to eight-cell-stage diploid embryos from *Frs2α*$^{+/-}$ intercrosses were aggregated with wild-type tetraploid embryos at the four-cell stage, cultured to the blastocyst stage, and then transplanted to foster mothers for development to E8.5. We recovered 8 heterozygous, 6 wild-type, and 2 homozygous embryos. All chimeras derived from diploid *Frs2α*$^{+/+}$ or *Frs2α*$^{+/-}$ embryonic cells had well-developed head folds, 4 to 7 somites, and an allantois (Fig. 5A). Chimeras derived from *Frs2α*$^{-/-}$ diploid embryonic cells developed head folds, but these had an abnormal shape (Fig. 5B). Furthermore, these chimeras did not develop somites or an allantois. Although the *Frs2α*$^{-/-}$ 2N<-> wild-type 4N chimeras did not complete gastrulation, they did morphologically establish an A-P axis. Thus, the block to A-P axis formation in
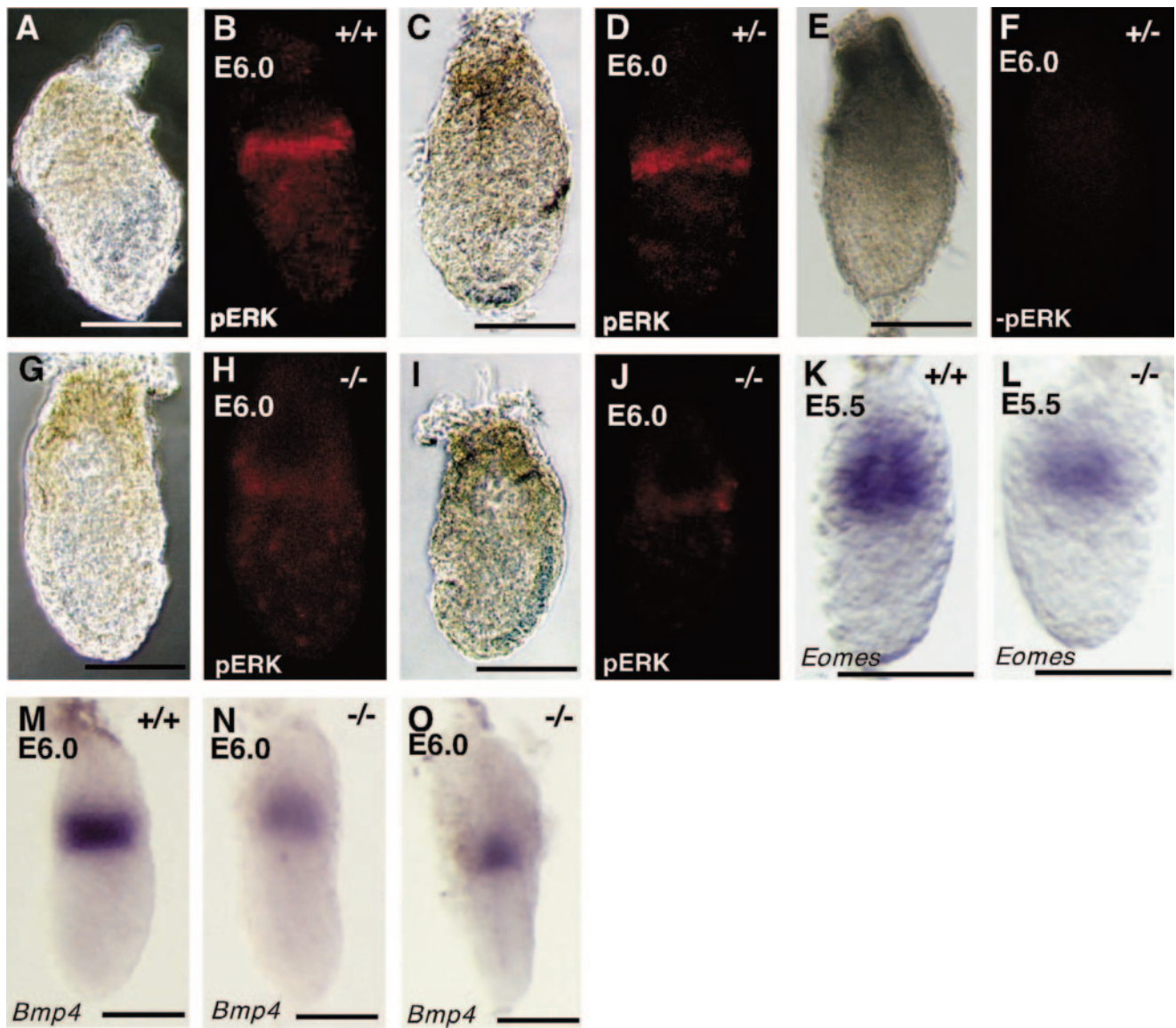
FIG. 3. Activation of Erk and expression of marker genes in ExE of *Frs2α*-null embryos at E5.5 and E6.0. Embryonic stage, genotype, and marker gene are indicated for each image. Whole-mount antibody staining: bright-field images (A, C, E, G, and I) followed by corresponding fluorescent images (B, D, F, H, and J). Control samples without primary antibodies are shown in panels E and F. Scale bars, 100 μm.

the *Frs2α*-null embryos appears to reside in the extraembryonic tissues including the ExE, the major site of *Frs2α* expression, but not in the epiblast.

The abnormal head folds and the absence of somites and allantois in the *Frs2α*$^{-/-}$ 2N <-> wild-type 4N chimeras indicate that FRS2α likely plays a role in gastrulation as well. To examine the role of *Frs2α* in gastrulation, chimeras were constructed by injecting *Frs2α*$^{-/-}$ ES cells, constitutively expressing LacZ, into wild-type diploid blastocysts. In such chimeras, ES cells exclusively colonize the epiblast and its derivatives, whereas cells from the host blastocysts will colonize both the epiblast and extraembryonic tissues (42). From embryos recovered at E7.5, we obtained chimeras exhibiting a wide range of *Frs2α*$^{-/-}$ ES cell contribution. In several chimeras with a low contribution of donor ES cells, LacZ (+) *Frs2α*$^{-/-}$ cells were often found in the primitive streak (Fig. 5C). Although many mutant cells were present in the epiblast and the ectodermal layer of the amnion, few mutant cells were found in embryonic mesoderm (Fig. 5D to F). Transverse sections of the chimeras with a high contribution of mutant cells revealed the presence of a well-defined primitive streak at E7.5 (Fig. 5F and G). Thus, as observed in the tetraploid chimeras, wild-type extraembryonic tissues, i.e., the ExE, can rescue A-P axis formation in a largely *Frs2α*$^{-/-}$ epiblast. The transverse sections also show an accumulation of a large number of mutant cells within the streak, suggesting that *Frs2α*$^{-/-}$ cells are impaired in their ability to move through the streak (Fig. 5F and G). Consistent with a requirement for *Frs2α* in cells traversing the primitive streak, *Frs2α* expression was detected in the primitive streak of E7.5 embryos by in situ hybridization (data not shown).
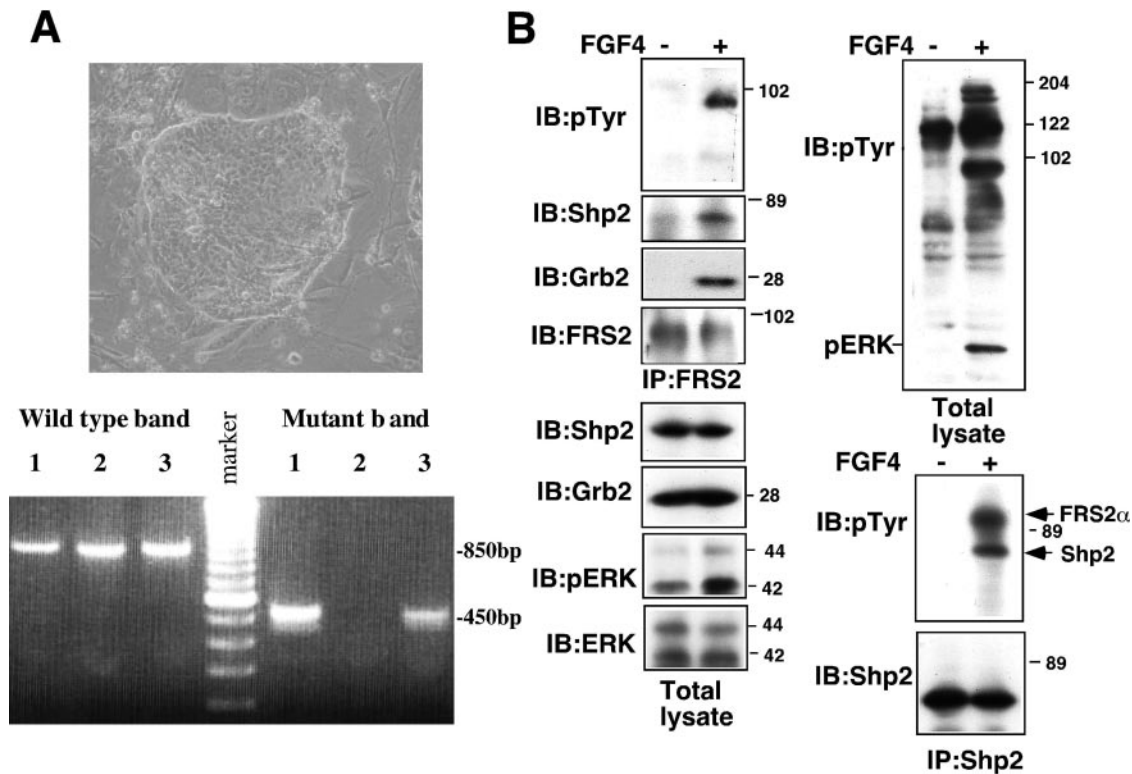
FIG. 4. Activation of signaling pathways through FRS2α in TS cells in response to FGF4 stimulation. (A) Morphology of a wild-type TS colony (upper panel) and PCR genotyping (lower panel). Each line indicates individual TS colonies. The genotypes indicated in lanes 1 and 3 were heterozygotes, and that indicated in lane 2 was wild type. (B) TS cells were starved in 0.5% serum overnight, stimulated with FGF4 (100 ng/ml) and heparin (5 μg/ml) for 10 min, lysed, and subjected to immunoprecipitation (IP) as indicated. The samples were resolved by sodium dodecyl sulfate-polyacrylamide gel electrophoresis and immunoblotted (IB) with several antibodies as indicated.

Decreased expression of *Bmp4* and *Nodal* and reduced Smad activation in *Frs2α*$^{-/-}$ embryos. We next examined the expression of *Bmp4* and *Eomesodermin* (*Eomes*) transcripts, both of which are normally expressed in ExE at the egg cylinder stage, E6.0 (23, 35) (Fig. 3K and M). The experiment presented in Fig. 3K to O shows that the expression of *Bmp4* and *Eomes* was decreased in mutant embryos. Therefore, we next asked whether FGF4 regulates *Bmp4* expression in cultured TS cells. We found that following FGF4 deprivation, *Bmp4* expression was markedly downregulated, reaching basal levels within 12 h. Under the same conditions of FGF4 deprivation, *Fgfr2* expression was gradually decreased but detected at the significant levels after 36 h (Fig. 6A). On the other hand, *Bmp4* expression was rapidly and strongly induced in response to FGF4 stimulation (Fig. 6B). In addition, *Bmp4* expression was reduced

when, prior to FGF4 stimulation, TS cells were pretreated with the specific MEK (MAPK kinase [MAPKK]) inhibitor PD98059 to inhibit activation of MEK-MAP kinase cascade (Fig. 6B). Thus, expression of *Bmp4* appears tightly regulated by FGF4 in TS cells. As FRS2α is a critical mediator of the FGF-induced MAP kinase response in the ExE (Fig. 3B to J), this finding is consistent with a role for FRS2α in FGF4 stimulation of *Bmp4* expression in TS cells.

To further explore the mechanism of FGF4-induced expression of *Bmp4* in TS cells, we examined *Bmp4* promoter activity. The mouse *Bmp4* gene possesses three known promoters that are utilized predominantly in a cell type-specific manner (designated 1A, 1B, and intron 2 in Fig. 6C) (12, 22, 45). To measure FGF4-induced activity of these promoters in TS cells, we ligated either a 2.5-kb fragment of the 5′-flanking region containing the 1A promoter (construct 1A), intron 1 containing the 1B promoter (construct 1B), or intron 2 containing the intron 2 promoter (construct 2) to a promoterless luciferase reporter gene. We found increased transcriptional activity with construct 2, but all the constructs, including construct 2, showed no significant difference in activity in response to FGF4 stimulation. This finding suggests that the intron 2 promoter, but not the 1A or 1B promoter, is utilized in TS cells. To determine whether an FGF4-responsive regulatory region is located in an upstream 5′-flanking sequence, we ligated a 1.4-kb fragment of the upstream 5′-flanking region (construct

TABLE 1. Isolation of TS cell lines derived from blastocysts obtained by heterozygous intercrossing[a]

Total no. of blastocysts	Attachment and outgrowth	No. of blastocysts from which TS cell lines were established	Genotype		
			+/+	+/−	−/−
19	19	14	5	9	0

[a] Whereas 14 +/+ or +/− blastocysts produced TS cell lines, no −/− blastocyst produced TS cell line (*P* = 0.0178).
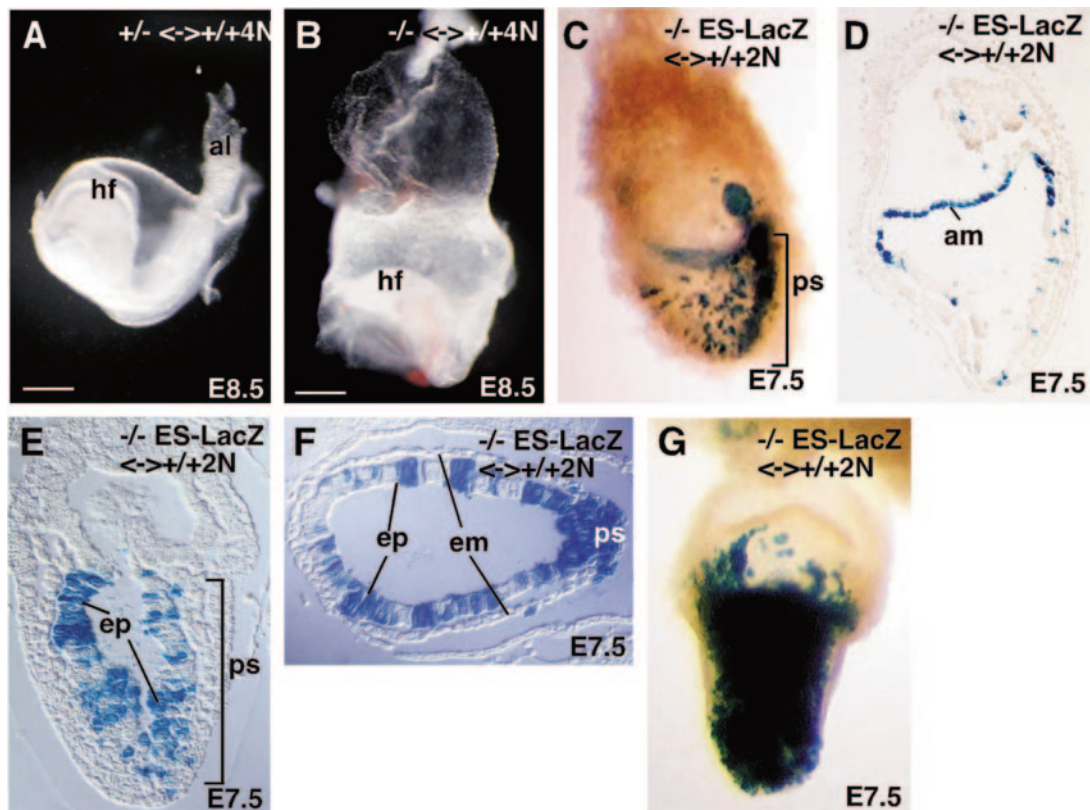
FIG. 5. Rescue of A-P patterning defects in $Frs2\alpha^{-/-}$ <-> wild-type 4N chimeric embryos and the presence of gastrulation defects in $Frs2\alpha^{-/-}$ ES cell <-> wild-type 2N chimeric embryos. Chimeric embryos recovered at E8.5 derived from $Frs2\alpha^{-/+}$ (A) or $Frs2\alpha^{-/-}$ (B) diploid and wild-type tetraploid morula aggregations. Chimeric embryos constructed by injection of $Frs2\alpha^{-/-}$ ES cells into 2N wild-type blastocysts were stained with LacZ at E7.5 (C to G). Transverse sections (F) and sagittal sections (D and E) of chimeric embryos. The sections in D and F were obtained from the embryos shown in C and G, respectively. Hf, head fold; al, allantois; ps, primitive streak; am, amnion; ep, epiblast; em, embryonic mesoderm.

5′) to the luciferase reporter gene containing the thymidine kinase (TK) minimal promoter (Fig. 6C). The results presented in Fig. 6D show that construct 5′ gave an approximately 3.5-fold increase in transcription in response to FGF4 stimulation. This finding suggests that an FGF4-responsive element resides in the sequence of the upstream 5′-flanking region (Fig. 6C). We found that FGF4 stimulation of the *Bmp4* promoter activity is blocked by the MEK inhibitor PD98059 (N. Gotoh, unpublished data), suggesting that ERK activity is required for stimulation of *Bmp4* transactivation. In addition, several consensus motifs for transactivating growth factors that are known to be activated by MAP kinase, such as AP-1, were found in the FGF4-responsive element of the *Bmp4* gene.

Bmp4 belongs to a family of tumor growth factor β-like ligands that activate Smad 1, 5, and 8, two of which, *Smad1* and *Smad5*, are expressed at the pregastrulation stage of mouse embryos (27). To explore the role of FRS2α in *Bmp4* signaling, we examined the activation of Smads 1 and 5 in embryos by immunohistochemistry using anti-phospho-Smad 1, 5, and 8 antibodies. We analyzed embryos at the prestreak and early-streak stages, before gross morphological or histological abnormalities are apparent in *Frs2α*-null embryos. In wild-type embryos, Smads 1 and 5 were strongly activated in a proximal to distal gradient within the epiblast (18) (Fig. 7B). In contrast, activation of Smads 1 and 5 was weak in FRS2α-deficient embryos (Fig. 7D), while a similar amount and distribution of

Smad1/5 was found in wild-type and mutant embryos (data not shown). These results are consistent with Bmp4, expressed on the distal rim of ExE, activating Bmp receptors in the epiblast and triggering the phosphorylation of Smads 1 and 5. In FRS2α-deficient embryos, the decreased levels of *Bmp4* expression would then lead to reduced Smad 1 and 5 phosphorylation in mutant embryos.

We also compared the expression of *Nodal* and its cofactor *Cripto* in mutant and wild-type embryos. *Nodal* and *Cripto* transcripts are localized to the posterior proximal epiblast of E6.5 wild-type embryos (Fig. 7G and I) (11, 47, 48). Decreased levels of *Nodal* and *Cripto* expression were observed in *Frs2α* mutants; furthermore both transcripts were not localized to the posterior proximal epiblast but are rather symmetrically distributed (Fig. 7H and J). These experiments raise the possibility that the primary defect in FRS2α-deficient ExE may contribute secondarily to aberrant expression of *Nodal* and *Cripto* in the epiblast.

DISCUSSION

In this report we demonstrate that FRS2α plays a critical role in several steps during mouse embryogenesis.

FRS2α is essential for maintenance of TS cells in the ExE. Experiments are presented demonstrating that FRS2α is essential for FGF4-dependent maintenance of self-renewing TS
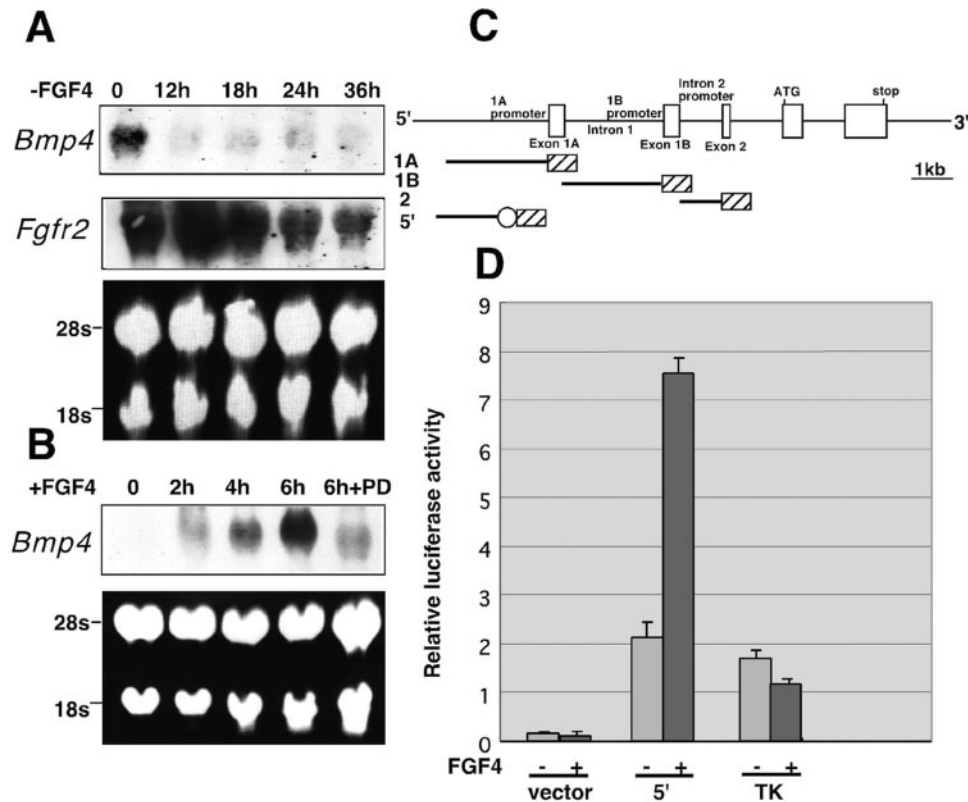
FIG. 6. FGF4 stimulation of *Bmp4* expression in TS cells and transcriptional activity of *Bmp4* promoters. (A) Total RNA was prepared from the TS cells at the indicated time points after deprivation of FGF4, heparin, and EMFI-CM. (B) TS cells were starved in 2% serum for 8 h with or without pretreatment with 50 μM the MEK inhibitors PD98059 for 30 min, stimulated with FGF4 (100 ng/ml) and heparin (5 μg/ml) for the indicated time points, and lysed for extraction of total RNA. (A and B) The RNA samples were subjected to Northern blotting with probes specific for *Bmp4* or *Fgfr2*. The 5′-flanking region of the mouse *Bmp4* gene confers FGF4-induced activation of transcription. (C) Schematic representation of the mouse *Bmp4* gene and constructs used for measuring transcriptional activity. Hatched boxes indicate a luciferase reporter gene. An open circle indicates the TK minimal promoter. (D) The results of transcriptional activity measurements obtained from at least three separate transfections. TK indicates a construct carrying only the TK minimal promoter fused to the luciferase reporter gene.

cells. In wild-type embryos, pronounced MAPK activation was detected in the ExE region, where TS cells reside. However, marked reduction of MAPK activation was observed in FRS2α deficient mutant embryos (Fig. 3A to J). While FGF4 stimulation leads to the formation of wild-type TS colonies, we have shown that Frs2α$^{-/-}$ TS colonies that appear after the first passage die within five passages. This experiment shows that the integrity of FRS2α is required for FGF4 stimulation of TS colonies and that signaling pathways that are dependent upon FRS2α are required for the survival and/or self-renewal of TS cells. The loss of function of TS cells in the ExE may be the main cause of death of mutant embryos.

Blastocyst stage embryos are composed of three different cell types: inner cell mass (ICM), primitive endoderm, and trophectoderm (46). After implantation, the ICM forms the epiblast and the primitive endoderm differentiates into the visceral and parietal endoderm layers of the yolk sac. Meanwhile, the polar trophectoderm overlying the ICM develops into ExE, ectoplacental cone, and secondary giant cells, all precursors to the trophoblast tissues, the fetal portion of the placenta (34). It has been proposed that the preimplantation ICM and the postimplantation epiblast produce FGF4, which maintains self-renewal of TS cells in the overlying polar tro-

phoectoderm and ExE, respectively (34, 43). As TS cells move away from the source of FGF4 in the ICM/epiblast, they progressively differentiate into ectoplacental cone and trophoblast giant cells. Similarly in culture, TS cells can self-renew in the presence of FGF4, but they differentiate into polyploid giant cells upon FGF4 deprivation. The developmental arrest of *Fgf4*-null embryos at the peri-implantation stage likely results from a failure to generate differentiated trophoblast tissues due to the loss of TS cells (13). In fact, some of the *Frs2α*-null embryos died around implantation. Other mutants were not phenotypically discernible prior to the onset of gastrulation, but the majority of these generally had degenerated by E8.5. The more advanced *Frs2α* mutants were observed in crosses between mice of a mixed genetic background (129sv/EV and Swiss Webster); thus, the variability in viability may reflect the presence of modifier loci. Such loci may promote the transient production and/or survival of TS cells, potentially through FRS2α-independent intracellular signaling pathways.

Because *Fgf4* and several *Fgfr* isoforms are expressed in *Frs2α*-null embryos, FRS2α-independent signaling pathways could still operate. FRS2α promotes MAPK activation through complex formation with Shp2 and Grb2, enabling tyrosine phosphorylation of Shp2 by activated FGFRs (Fig. 4B). Al-
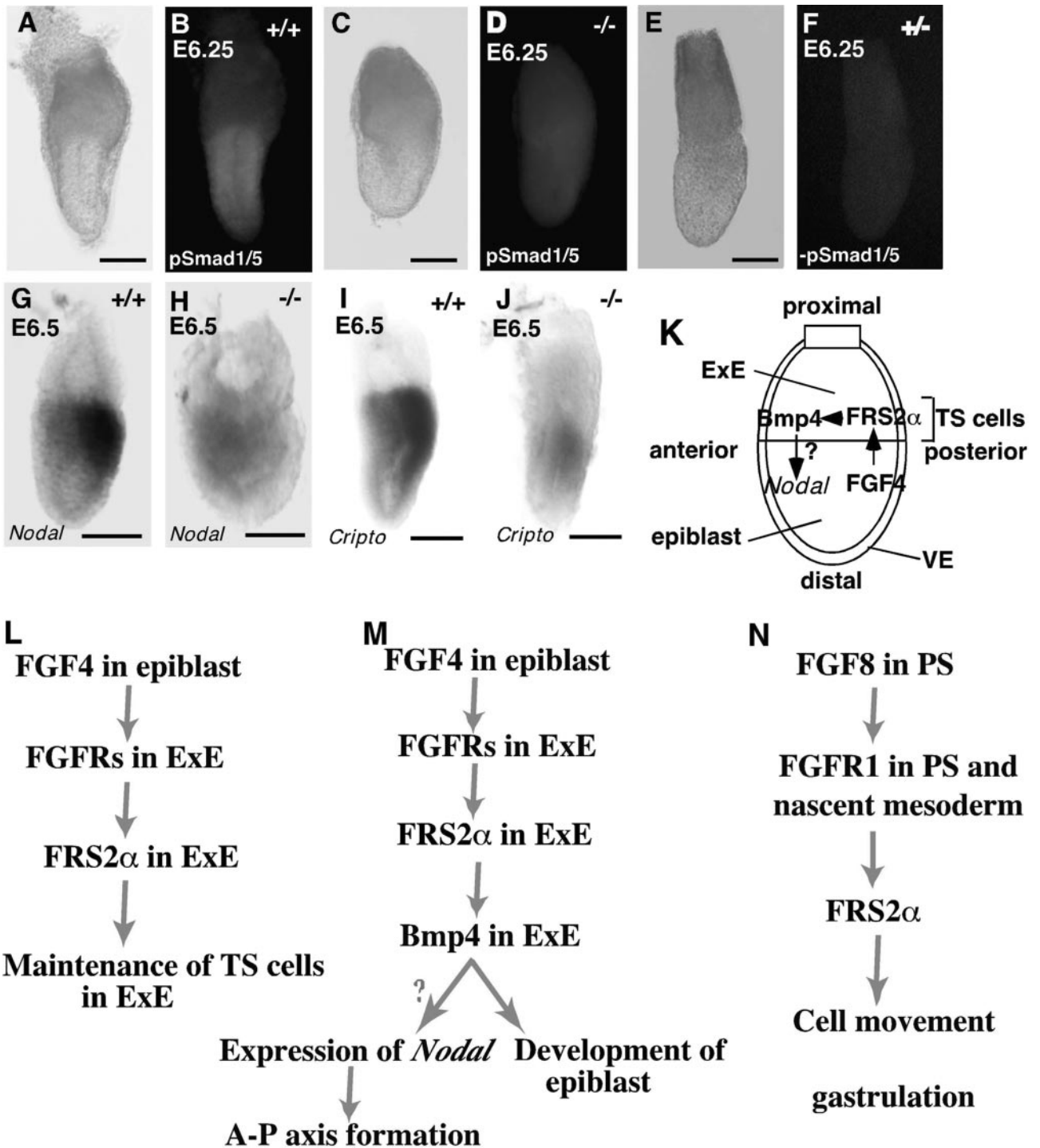
FIG. 7. Expression of marker genes and activation of Smads in epiblast of *Frs2α*-null embryos at E6.0 to 6.5. Embryonic stage, genotype, and marker gene are indicated for each image. All embryos are oriented with anterior side to the left. Whole-mount antibody staining: bright-field images (A, C, and E) followed by corresponding fluorescent images (B, D, and F). Control samples without primary antibodies are shown in panels E and F. Whole-mount in situ hybridization (G to J). Scale bars, 100 μm. Multiple functions of FRS2α during early embryogenesis. (L) FRS2α is essential for FGF4 stimulation of maintenance of self-renewing TS cells in the ExE. At the egg cylinder stage, FGF4 produced in epiblast stimulates FGFRs expressed in ExE resulting in recruitment and tyrosine phosphorylation of FRS2α. Signaling pathways that are dependent on FRS2α are required for proliferation of self-renewing TS cells in ExE to develop trophoblast lineage. (K and M) A hypothetical connection between FGF and Bmp4 signaling mediated by FRS2α. FGF4 stimulation of FGFRs that are expressed in ExE leads to recruitment and tyrosine phosphorylation of FRS2α. As FRS2α is required for expression of *Bmp4* in ExE, it is postulated that Bmp4 functions as a paracrine factor in ExE that contributes towards the induction and maintenance of *Nodal* expression in the proximal epiblast and towards the development of the epiblast. (N) FRS2α plays a role in cell movements through the primitive streak during gastrulation. FGF8 stimulation of FGFR1 and other FGFRs that may be expressed in the primitive streak (PS) and nascent mesoderm leads to recruitment and tyrosine phosphorylation of FRS2α. Signaling pathways that are dependent on FRS2α are required for cell movement through the primitive streak during gastrulation.

though FRS2α plays a role in MAPK stimulation, a diminished and transient FGF1-induced MAPK response can be detected in $Frs2\alpha^{-/-}$ mouse embryonic fibroblasts (MEFs) (16). Furthermore, it was shown that Shp2 can mediate, at least partially, MAPK activation even in the absence of both of its tyrosine phosphorylation sites (2). Moreover, FGF1 stimulation of tyrosine phosphorylation of Shc, resulting in Ras/MAPK stimulation, may provide an alternative route for FGF1-induced MAPK stimulation in $Frs2\alpha^{-/-}$ MEFs. FGF1-stimulation of phospholipase C-γ (PLCγ) activation, followed by Ca^{+2} release and protein kinase-C (PKC) stimulation, are preserved in $Frs2\alpha^{-/-}$ MEFs. Both PLCγ and Shc are expressed in TS cells (data not shown), and therefore these signaling proteins may support partial FGF-signaling in $Frs2\alpha$-null embryos.

FRS2α plays a role in cell movement through the primitive streak during gastrulation. To examine the role of $Frs2\alpha$ during gastrulation, we constructed chimeras from $Frs2\alpha^{-/-}$ ES cells and diploid wild-type blastocysts. Similar to cellular defects present in $Fgfr1$- or $Fgf8$-null embryos (7, 10, 40, 52), the FRS2α-deficient cells are impaired in their ability to exit the primitive streak. This experiment suggests that, in addition to the requirement of FRS2α in FGF4-signaling in ExE, the docking protein also functions as an intracellular mediator of signaling pathways, stimulated by FGF8 and FGFR1 during gastrulation (Fig. 7N). It should be noted that Shp2, one of the effectors of FRS2α, has been shown to play a role in cell migration through primitive streak (37).

A potential FRS2α-mediated link between FGF, Bmp4, and Nodal signaling pathways. We have shown that the expression of $Bmp4$ is decreased in $Frs2\alpha^{-/-}$ embryos and that FGF4 stimulation leads to enhanced expression of $Bmp4$ in TS cells (Fig. 3N and O and 6B). Moreover, the expression of $Bmp4$ is rapidly down-regulated after removal of FGF4 from TS cells (Fig. 6A). Although correlative and indirect, these findings suggest that FGF4 signaling contributes to $Bmp4$ gene regulation in ExE. Indeed, it appears that a FGF4 responsive element is located in the 5′-flanking region of the mouse $Bmp4$ gene (Fig. 6C and D).

The $Frs2\alpha$-null embryos show defects in transformating the P-D axis of the egg cylinder into the A-P axis of the gastrula (Fig. 1F, H, and J and 2). As the P-D to A-P rotation always occurs before the appearance of nascent mesoderm in wild-type embryos, the detection of mesoderm-like cells in $Frs2\alpha$ mutants, suggests that they develop beyond the time the A-P axis formation. Thus, FRS2α dependent FGF-signaling may also contribute towards the establishment of the A-P axis.

The Nodal signaling pathway plays a central role in a number of developmental events in the early postimplantation embryo: the establishment of the P-D axis, rotation of the AVE and organization of the A-P axis, mesoderm and endoderm formation, and left-right (L-R) patterning. It has been shown that $Nodal$ expression is initially induced in the proximal epiblast by an unknown stimulus, thought to be produced at approximately E5.0 by the ExE (31, 48). A Nodal signaling cascade is then amplified by a positive feedback loop that involves its own enhancer sequence, termed ASE, and an enhancer binding factor FoxH1 (6, 31, 36). $Nodal$ expression is propagated throughout the epiblast, and then Nodal acts on the overlying distal VE to induce the expression of genes required

for AVE formation, rotation, and function. Once the AVE is specified on the anterior side of the egg cylinder, expression of $Nodal$ becomes confined to the proximal posterior side of epiblast to promote mesoderm and endoderm production by the primitive streak. Nodal acts in a dosage-dependent manner to execute these different steps in embryonic patterning (24, 30). In the absence of Nodal, patterning along the P-D axis does not occur and no AVE precursor forms at the distal tip of the egg cylinder (6). Low doses of Nodal signaling, achieved through hypomorphic alleles, induce the AVE distally but do not support its anterior migration. At slightly higher, but still subnormal levels of Nodal, the embryos properly complete gastrulation but fail to correctly establish the L-R axis.

It is noteworthy that the absence of AVE rotation in $Frs2\alpha$-null embryos strikingly resembles the phenotype observed in embryos expressing hypomorphic alleles of $Nodal$ (23). Other mutations thought to reduce the level of Nodal signaling also disrupt gastrulation by obstructing rotation of the AVE. These include mutants lacking $Cripto$, a positive cofactor for Nodal and mutants deficient in $FoxH1$ (11, 30, 53).

The decreased expression of $Nodal$ in the $Frs2\alpha$-null mutants at E6.5 raises the possibility that the absence of AVE rotation may result from insufficient levels of Nodal signaling. In this study, we showed the phenotype of $Frs2\alpha$-null embryos in a mixed genetic (129sv/Ev × Swiss Webster) background. We also analyzed $Frs2\alpha$-null mutants in a 129sv/EV inbred background and found that the mutant embryos showed reduced levels of expression of $Brachyury$ and $Cer-1$ and very little levels of expression of $Nodal$ at E6.0 to 6.5, suggestive of a defect in the P-D axis formation (data not shown). This phenotype is more severe than those described in this study, in association with more reduced levels of expression of $Nodal$.

$Bmp4$-null embryos have a variety of phenotypes, underscoring the multiple roles of Bmp4 during embryogenesis. $Bmp4^{-/-}$ embryos on the C57BL/6 background are developmentally retarded at E7.5; mutant embryos lack an organized primitive streak and produce only a small amount of extraembryonic mesoderm (50). This phenotype is similar to that of $Frs2\alpha$-null embryos, hinting of a possible functional link between FRS2α and Bmp4 signaling in pre- and early-streak-stage embryos. We analyzed expression of $Cer-1$, Hex, and $Nodal$ in the $Bmp4^{-/-}$ embryos and found that these were expressed at very low levels, similar to those of the $Nodal$-null embryos or $Frs2\alpha$-null embryos in a 129sv/EV background (data not shown) (6).

On the basis of these findings, it appears that FRS2α plays a role in FGF4 stimulation of $Bmp4$ expression in ExE. Acting as a paracrine factor, Bmp4 may, accordingly, contribute to the induction and maintenance of $Nodal$ expression in the proximal epiblast and development of epiblast (Fig. 7K and M). Bmp4 might be an initial stimulus to induce expression of $Nodal$ in the proximal epiblast.

In summary, the experiments presented in this report demonstrate that loss of FRS2α impairs at least two critical processes in the development of extraembryonic and embryonic tissues in the early postimplantation stage mouse embryo. We demonstrate that FRS2α is essential for FGF4-dependent maintenance of self-renewing TS cells in the ExE (Fig. 7L) and that FRS2α may play a critical role in cell movement through the primitive streak during gastrulation (Fig. 7N). Our exper-

iments also suggest a potential new link between FGF signaling and *Bmp4* and *Nodal* signaling pathways to promote A-P axis formation (Fig. 7K and M).

ACKNOWLEDGMENTS

REFERENCES

1. **Ang, S. L., R. A. Conlon, O. Jin, and J. Rossant.** 1994. Positive and negative signals from mesoderm regulate the expression of mouse Otx2 in ectoderm explants. Development **120:**2979–2989.
2. **Araki, T., H. Nawa, and B. G. Neel.** 2003. Tyrosyl phosphorylation of Shp2 is required for normal ERK activation in response to some, but not all growth factors. J. Biol. Chem. **278:**41677–41684.
3. **Arman, E., R. Haffner-Krausz, Y. Chen, J. K. Heath, and P. Lonai.** 1998. Targeted disruption of fibroblast growth factor (FGF) receptor 2 suggests a role for FGF signaling in pregastrulation mammalian development. Proc. Natl. Acad. Sci. USA **95:**5082–5087.
4. **Beddington, R. S., and E. J. Robertson.** 1998. Anterior patterning in mouse. Trends Genet. **14:**277–284.
5. **Belo, J. A., T. Bouwmeester, L. Leyns, N. Kertesz, M. Gallo, M. Follettie, and E. M. De Robertis.** 1997. Cerberus-like is a secreted factor with neutralizing activity expressed in the anterior primitive endoderm of the mouse gastrula. Mech. Dev. **68:**45–57.
6. **Brennan, J., C. C. Lu, D. P. Norris, T. A. Rodriguez, R. S. Beddington, and E. J. Robertson.** 2001. Nodal signaling in the epiblast patterns the early mouse embryo. Nature **411:**965–969.
7. **Ciruna, B. G., L. Schwartz, K. Harpal, T. P. Yamaguchi, and J. Rossant.** 1997. Chimeric analysis of fibroblast growth factor receptor-1 (Fgfr1) function: a role for FGFR1 in morphogenetic movement through the primitive streak. Development **124:**2829–2841.
8. **Corson, L. B., Y. Yamanaka, K.-M. V. Lai, and J. Rossant.** 2003. Spatial and temporal patterns of ERK signaling during mouse embryogenesis. Development **130:**4527–4537.
9. **Crossley, P. H., and G. R. Martin.** 1995. The mouse Fgf8 gene encodes a family of polypeptides and is expressed in regions that direct outgrowth and patterning in the developing embryo. Development **121:**439–451.
10. **Deng, C. X., A. Wynshaw-Boris, M. M. Shen, C. Daugherty, D. M. Ornitz, and P. Leder.** 1994. Murine FGFR-1 is required for early postimplantation growth and axial organization. Genes Dev. **8:**3045–3057.
11. **Ding, J., L. Yang, Y. T. Yan, A. Chen, N. Desai, Wynshaw-Boris, A., and M. M. Shen.** 1998. Cripto is required for correct orientation of the anterior-posterior axis in the mouse embryo. Nature **395:**702–707.
12. **Ebara, S., S. Kawasaki, I. Nakamura, T. Tsutsumimoto, K. Nakayama, T. Nikaido, and K. Takaoka.** 1997. Transcriptional regulation of the *mBMP-4* gene through an E-box in the 5′-flanking promoter region involving USF. Biochem. Biophys. Res. Commun. **240:**136–141.
13. **Feldman, B., W. Poueymirou, V. E. Papaioannou, T. M. DeChiara, and M. Goldfarb.** 1995. Requirement of FGF-4 for postimplantation mouse development. Science **267:**246–249.
14. **Givol, D., V. P. Eswarakumar, and P. Lonai.** 2003. Molecular and cellular biology of FGF signaling, p. 367–379. *In* C. J. Epstein, R. P. Erickson, and A. Wynshaw-Boris. (ed.), Inborn errors of development: the molecular basis of clinical disorders of morphogenesis. Oxford University Press, New York, N.Y.
15. **Gotoh, N., S. Laks, M. Nakashima, I. Lax, and J. Schlessinger.** 2004. FRS2 family docking proteins with overlapping roles in activation of MAP kinase have distinct spatial-temporal patterns of expression of their transcripts. FEBS Lett. **564:**14–18.
16. **Hadari, Y. R., N. Gotoh, H. Kouhara, I. Lax, and J. Schlessinger.** 2001. Critical role for the docking-protein FRS2 alpha in FGF receptor-mediated signal transduction pathways. Proc. Natl. Acad. Sci. USA **98:**8578–8583.

17. **Hadari, Y. R., H. Kouhara, I. Lax, and J. Schlessinger.** 1998. Binding of Shp2 tyrosine phosphatase to FRS2 is essential for fibroblast growth factor-induced PC12 cell differentiation. Mol. Cell. Biol. **18:**3966–3973.
18. **Hayashi, K., T. Kobayashi, T. Umino, R. Goitsuka, Y. Matsui, and D. Kitamura.** 2002. SMAD1 signaling is critical for initial commitment of germ cell lineage from mouse epiblast. Mech. Dev. **118:**99–109.
19. **Hermesz, E., S. Mackem, and K. A. Mahon.** 1996. Rpx: a novel anterior-restricted homeobox gene progressively activated in the prechordal plate, anterior neural plate and Rathke's pouch of the mouse embryo. Development **122:**41–52.
20. **Hoodless, P. A., M. Pye, C. Chazaud, E. Labbe, L. Attisano, J. Rossant, and J. L. Wrana.** 2001. FoxH1 (Fast) functions to specify the anterior primitive streak in the mouse. Genes Dev. **15:**1257–1271.
21. **Kouhara, H., Y. R. Hadari, T. Spivak-Kroizman, J. Schilling, D. Bar-Sagi, I. Lax, and J. Schlessinger.** 1997. A lipid-anchored Grb2-binding protein that links FGF-receptor activation to the Ras/MAPK signaling pathway. Cell **89:**693–702.
22. **Kurihara, T., K. Kitamura, K. Takaoka, and H. Nakazato.** 1993. Murine bone morphogenetic protein-4 gene: existence of multiple promoters and exons for the 5′-flanking region. Biochem. Biophys. Res. Commun. **192:**1049–1056.
23. **Lawson, K. A., N. R. Dunn, B. A. Roelon, L. M. Zeinstra, A. M. Davis, C. V. Wright, J. P. Korving, and B. L. Hogan.** 1999. Bmp4 is required for the generation of primordial germ cells in the mouse embryo. Gene Dev. **13:**424–436.
24. **Lowe, A. L., S. Yamada, and M. R. Kuehn.** 2001. Genetic dissection of nodal function in patterning the mouse embryo. Development **128:**1831–1843.
25. **Luckow, B., and G. Schütz.** 1987. CAT constructions with multiple unique restriction sites for the functional analysis of eukaryotic promoters and regulatory elements. Nucleic Acids Res. **15:**5490.
26. **Manova, K., V. De Leon, M. Angeles, S. Kalantry, M. Giarre, L. Attisano, J. Wrana, and R. F. Bachvarova.** 1995. mRNAs for activin receptors II and IIB are expressed in mouse oocytes and in the epiblast of pregastrula and gastrula stage mouse embryos. Mech. Dev. **49:**3–11.
27. **Massague, J., S. W. Blain, and R. S. Lo.** 2000. TGFbeta signaling in growth control, cancer, and heritable disorders. Cell **103:**295–309.
28. **Nagy, A., E. Gocza, E. M. Diaz, V. R. Prideaux, E. Ivanyi, M. Markkula, and J. Rossant.** 1990. Embryonic stem cells alone are able to support fetal development in the mouse. Development **110:**815–821.
29. **Niswander, L., and G. R. Martin.** 1992. Fgf-4 expression during gastrulation, myogenesis, limb and tooth development in the mouse. Development **114:**755–768.
30. **Norris, D. P., J. Brennan, E. K. Bikoff, and E. J. Robertson.** 2002. The Foxh1-dependent autoregulatory enhancer controls the level of Nodal signals in the mouse embryo. Development **129:**3455–3468.
31. **Norris, D. P., and E. J. Robertson.** 1999. Asymmetric and node-specific nodal expression patterns are controlled by two distinct cis-acting regulatory elements. Genes Dev. **13:**1575–1588.
32. **Ong, S. H., G. R. Guy, Y. R. Hadari, S. Laks, N. Gotoh, J. Schlessinger, and I. Lax.** 2000. FRS2 proteins recruit intracellular signaling pathways by binding to diverse targets on fibroblast growth factor and nerve growth factor receptors. Mol. Cell. Biol. **20:**979–989.
33. **Ornitz, D. M., and N. Itoh.** 2001. Fibroblast growth factors. Genome Biol. Rev. **2:**1–9.
34. **Rossant, J., and J. C. Cross.** 2001. Placental development: lessons from mouse mutants. Nat. Rev. Genet. **2:**538–548.
35. **Russ, A. P., S. Wattler, W. H. Colledge, S. A. Aparicio, M. B. Carlton, J. J. Pearce, S. C. Barton, M. A. Surani, K. Ryan, M. C. Nehls, V. Wilson, and M. J. Evans.** 2000. Eomesodermin is required for mouse trophoblast development and mesoderm formation. Nature **404:**95–99.
36. **Saijoh, Y., H. Adachi, R. Sakuma, C. Y. Yeo, K. Yashiro, M. Watanabe, H. Hashiguchi, K. Mochida, S. Ohishi, M. Kawabata, K. Miyazono, M. Whitman, and H. Hamada.** 2000. Left-right asymmetric expression of lefty2 and nodal is induced by a signaling pathway that includes the transcription factor FAST2. Mol. Cell **5:**35–47.
37. **Saxton, T. M., B. G. Ciruna, D. Holmyard, S. Kulkarni, K. Harpal, J. Rossant, and T. Pawson.** 2000. The SH2 tyrosine phosphatase shp2 is required for mammalian limb development. Nat. Genet. **24:**420–423.
38. **Schlessinger, J.** 2000. Cell signaling by receptor tyrosine kinases. Cell **103:**211–225.
39. **Shawlot, W., and R. R. Behringer.** 1995. Requirement for Lim1 in head-organizer function. Nature **374:**425–430.
40. **Sun, X., E. N. Meyers, M. Lewandoski, and G. R. Martin.** 1999. Targeted disruption of Fgf8 causes failure of cell migration in the gastrulating mouse embryo. Genes Dev. **13:**1834–1846.
41. **Srinivas, S., T. Rodriguez, M. Clements, J. C. Smith, and R. S. Beddington.** 2004. Active cell migration drives the unilateral movements of the anterior visceral endoderm. Development **131:**1157–1164.
42. **Tam, P. P., and J. Rossant.** 2003. Mouse embryonic chimeras: tools for studying mammalian development. Development **130:**6155–6163.
43. **Tanaka, S., T. Kunath, A. K. Hadjantonakis, A. Nagy, and J. Rossant.** 1998.

Promotion of trophoblast stem cell proliferation by FGF4. Science **282:**2072–2075.

44. **Thomas, P. Q., A. Brown, and R. S. Beddington.** 1998. Hex: a homeobox gene revealing peri-implantation asymmetry in the mouse embryo and an early transient marker of endothelial cell precursors. Development **125:**85–94.

45. **Thompson, D. L., L. M. Gerlach-Bank, K. F. Barald, and R. J. Koenig.** 2003. Retionic acid repression of bone morphogenetic protein 4 in inner ear development. Mol. Cell. Biol. **23:**2277–2286.

46. **Tomihara-Newberger, C., O. Haub, H. G. Lee, V. Soares, K. Manova, and E. Lacy.** 1998. The amn gene product is required in extraembryonic tissues for the generation of middle primitive streak derivatives. Dev. Biol. **204:**34–54.

47. **Varlet, I., J. Collignon, and E. J. Robertson.** 1997. Nodal expression in the primitive endoderm is required for specification of the anterior axis during mouse gastrulation. Development **124:**1033–1044.

48. **Whitman, M.** 2001. Nodal signaling in early vertebrate embryos: themes and variations. Dev. Cell. **1:**605–617.

49. **Wilkinson, D. G., S. Bhatt, and B. G. Herrmann.** 1990. Expression pattern of the mouse T gene and its role in mesoderm formation. Nature **343:**657–659.

50. **Winnier, G., M. Blessing, P. A. Labosky, and B. L. Hogan.** 1995. Bone morphogenetic protein-4 is required for mesoderm formation and patterning in the mouse. Genes Dev. **9:**2105–2116.

51. **Xu, X., M. Weinstein, C. Liu, M. Naski, R. I. Cohen, D. M. Ornitz, P. Leder, and C. Deng.** 1998. Fibroblast growth factor receptor 2 (FGFR2)-mediated reciprocal regulation loop between FGF8 and FGF10 is essential for limb induction. Development **125:**753–765.

52. **Yamaguchi, T. P., K. Harpal, M. Henkemeyer, and J. Rossant.** 1994. fgfr-1 is required for embryonic growth and mesodermal patterning during mouse gastrulation. Genes Dev. **8:**3032–3044.

53. **Yamamoto, M., C. Meno, Y. Sakai, H. Shiratori, K. Mochida, Y. Ikawa, Y. Saijoh, and H. Hamada.** 2001. The transcription factor FoxH1 (FAST) mediates Nodal signaling during anterior-posterior patterning and node formation in the mouse. Genes Dev. **15:**1242–1256.

54. **Yamamoto, M., Y. Saijoh, A. Perea-Gomez, W. Shawlot, R. R. Behringer, S.-L. Ang, H. Hamada, and C. Meno.** 2004. Nodal antagonists regulate formation of the anteroposterior axis of the mouse embryo. Nature **428:**387–392.